Running the Gauntlet: Connectivity between spawning and nursery areas for arrowtooth flounder (*Atheresthes stomias*) in the Gulf of Alaska, as inferred from a biophysical individual-based model

William T. Stockhausen[a*], Kenneth O. Coyle[b], Albert J. Hermann[c,d], Deborah Blood[a], Miriam Doyle[a,c], Georgina A. Gibson[e], Sarah Hinckley[a,c], Carol Ladd[d], Carolina Parada[f,g]

[a]*Alaska Fisheries Science Center, National Marine Fisheries Service, NOAA, 7600 Sand Point Way NE, Seattle, WA 98115-6349.*
[b]*Institute of Marine Science, University of Alaska, Fairbanks, AK 99775-7220.*
[c]*Joint Institute for the Study of the Atmosphere and Ocean, University of Washington, Seattle WA 98195.*
[d]*NOAA/PMEL, 7600 Sand Point Way NE, Seattle, WA 98115-6349.*
[e]*International Arctic Research Center, University of Alaska Fairbanks, P.O. Box 757340, Fairbanks, AK 99775.*
[f]*Departamento de Geofísica, Universidad de Concepción, Casilla 160-C, Concepción, Chile.*
[g]*Instituto Milenio de Oceanografía, Universidad de Concepción, Concepción, Chile.*

ABSTRACT

Little is known regarding the early life transport and dispersion mechanisms, from offshore spawning areas to inshore nursery habitats, that potentially underlie recruitment variability for arrowtooth flounder in the Gulf of Alaska (GOA). We developed a biophysical individual-based model (IBM) for arrowtooth flounder early life history and dispersal with simple representations of swimming behavior, growth, and survival to explore the variability in connectivity between spawning and recruitment sites that can arise due solely to interannual variability in environmental forcing and its impact on transport. Results of our simulations for 1996-2011 show that, even in the absence of mortality, most (> 80%) individuals were unsuccessful in dispersing from presumed spawning areas along the continental shelf break to inshore nurseries in the GOA. For those that were successful, connectivity was directed in a counterclockwise fashion (southeast to northwest) following prevailing current patterns, with typical dispersion distances of 100s of km alongshore. The most productive spawning areas were in the southeastern GOA (areas off Sitka and Cross Sound), while the most effective nursery areas were in the central and western GOA (Prince William Sound and North Kodiak areas). Arrowtooth flounder from spawning areas in the western GOA were exported from the system and likely contribute little to the population in the GOA, but may provide recruits to populations in the Aleutian Islands or eastern Bering Sea. We developed a suite of potential recruitment indices based on the connectivity results; however, none of these appeared to reflect estimated (age-1) recruitment to the population from a stock assessment model.

Keywords (at least 4): USA, Alaska, Gulf of Alaska; Atheresthes stomias, arrowtooth flounder, recruitment; modelling

*Corresponding author.

E-mail address: william.stockhausen@noaa.gov (W. T. Stockhausen).

List of Abbreviations

Abbreviation	Description
AICc	Akaike Information Criterion, corrected for small sample size
AO	Arctic Oscillation
CGOA	Coastal Gulf of Alaska (ROMS model grid)
CSF	cross-shelf flow
DisMELS	Dispersal Model for Early Life Stages
ENSO	El Nino/Southern Oscillation
EOF	empirical orthogonal function
FOCI	Fisheries-Oceanography Coordinated Investigations
GOA	Gulf of Alaska
GOAIERP	Gulf of Alaska Integrated Ecosystem Research Project
IBM	individual-based model
LFPr	large feeding preflexion (larvae)
LYS	large yolk sac (larvae)
MEI	Multivariate ENSO Index
NMFS	National Marine Fisheries Service
NOAA	National Oceanic and Atmospheric Administration
NPRB	North Pacific Research Board
PC	principal component
PDO	Pacific Decadal Oscillation
POP	Pacific ocean perch
PWI	Prince of Wales Island
PWS	Prince William Sound
ROMS	Regional Ocean Modeling System
SFPr	small feeding preflexion (larvae)
SL	standard length
SYS	small yolk sac (larvae)

1. Introduction

The Gulf of Alaska Integrated Ecosystem Program (GOAIERP) is a vertically-integrated study of the physics, fisheries and ecosystem of the Gulf of Alaska (GOA). A principal goal of the GOAIERP is to identify how physical and biological variability affect recruitment of five commercially-and ecologically-important groundfish species in the GOA: arrowtooth flounder (*Atheresthes stomias*), Pacific ocean perch (*Sebastes alutus*), Pacific cod (*Gadus macrocephalus*), walleye pollock (*Gadus chalcogramma*), and sablefish (*Anaplopoma fimbria*). The working hypothesis adopted for the GOAIERP was that the survival of the earliest life stages of groundfishes, during transport from offshore natal areas to nearshore nursery habitats, is the principal influence affecting variability in subsequent recruitment to the population. As such, successful recruitment may be dependent on many interrelated factors affecting young groundfish along transport pathways from offshore natal areas to nearshore nursery habitats, including those directly influencing survival (such as food supply, competition and predation), as well as those influencing the physical environment and thus the pathways themselves (e.g. freshwater runoff, mixing and stratification, water temperature, and wind speed and direction). We refer to these biophysical processes occurring along, and influencing, the transport pathways during the first year of life as "the gauntlet".

The five focal groundfish species for the GOAIERP were chosen to provide a broad range of life history strategies across which to assess the importance of the gauntlet to understanding recruitment variability of groundfish stocks in the GOA. Arrowtooth flounder, the focus of this paper, is a pleuronectid flatfish species found on soft, muddy bottom on the continental shelf and slope and currently comprises the most abundant groundfish species in the

GOA (Matarese et al., 2003; Spies et al., 2015). They may live up to 34 years and range from central California north to the eastern Bering Sea, east along the Aleutian Islands and toward Cape Navarin, Russia, and along the east coast of Kamchatka and the Commander Islands (Blood et al., 2007). Arrowtooth flounder are found at depths from 12-900 m. In annual summer bottom trawl surveys conducted by the Alaska Fisheries Science Center (NOAA/NMFS), arrowtooth flounder are most often found between 300-500 m (Spies et al., 2015).

Various studies have found arrowtooth flounder spawning along the continental slope at depths between 100 and 500 m (Hirschberger and Smith, 1983), but most spawning occurs between 400-500 m (Blood et al., 2007). Spawning in the GOA probably begins in December and is substantially reduced by the end of February (Blood et al., 2007; Rickey, 1995). Females can produce 250,000-2,400,000 eggs per spawning season (Bouwens et al., 1999). Eggs are pelagic and the duration of the egg stage is temperature dependent. Most eggs and small larvae have been collected at >400 m depth, where hatching occurs (Blood et al., 2007). Late-stage eggs have been collected principally near troughs and canyons where downwelling relaxation and cross-shelf flow typically occur in winter (Blood et al., 2007). Newly hatched larvae possess a relatively large yolk sac; mean size at hatching is 4.4 mm standard length (SL; Blood et al. 2007). Yolk absorption is complete by 6.5-7 mm SL. Flexion occurs at 13.4 mm SL and transformation occurs about 45 mm SL (Blood et al., 2007; Bouwens et al., 1999). Larvae begin to ascend to shallower depths prior to complete yolk sac absorption. While most larvae are located along the outer shelf and slope, larger larvae tend to be further inshore and are associated with the deep-sea valleys and troughs that penetrate the shelf (Bailey and Picquelle, 2002). This association may provide enhanced transport pathways to nearshore nursery grounds. Interannual variation in size is small compared to intra-annual variation, suggesting that arrowtooth flounder hatch over an extended time period (Bouwens et al., 1999). Settlement to juvenile benthic nursery habitats starts at the beginning of August and finishes by the end of October.

Arrowtooth flounder play a key role in the GOA ecosystem as an important upper trophic level predator on walleye pollock and other forage fishes, as well as euphausiids, shrimp and cephalopods (Yang, 1993; Aydin et al., 2007). Estimated consumption of all forage fish (capelin, sandlance, eulachon, etc.) by adult arrowtooth flounder ranges from 0.3 to 1.2 million metric tons annually, while estimated consumption of pollock by adult arrowtooth ranges from 0.4 to 0.8 million metric tons. Annual consumption of euphausiids by adult arrowtooth is estimated to range from 0.1 to 0.8 million metric tons annually, with another 0.06-0.49 million metric tons consumed annually by juvenile arrowtooth flounder.

Historically, arrowtooth flounder in the GOA have not been targeted by a commercial fishery because their flesh degrades rapidly after being caught due to a proteolytic enzyme emitted from a myxoporean parasite that softens the flesh when heated (Spies et al., 2015). Recently developed processing techniques have, however, allowed a moderate commercial fishery to develop around Kodiak Island (http://www.afsc.noaa.gov/species/Arrowtooth_flounder.php).

The Gulf of Alaska is a dynamic ecosystem. Circulation in the GOA is predominantly east to west (counterclockwise). Along the continental shelf break of the northern GOA, the Alaskan Stream is a westward flowing boundary current with flow rates up to 80-100 cm s^{-1} (Reed, 1984). On the shelf, within about 50 km of the coast, the Alaska Coastal Current is a westward-flowing buoyancy-driven current (Royer, 1998; Stabeno et al., 2004) with flow rate of 25 to 175 cm s^{-1} (Johnson and Quinn, 1988; Stabeno et al., 2015a). In the eastern GOA, the wide and variable Alaska Current flows northward along the shelf break, while the Alaska Coastal Current flows northward along the shelf. The narrowness of the shelf in the eastern GOA results in strong interaction between the shelf-break flow and the coastal current (Stabeno et al., 2015b). Both the shelf-break currents and the coastal current can meander and shed eddies, affecting the trajectories and mixing of water masses (Bailey et al., 1997; Janout et al., 2009; Ladd and Stabeno, 2009; Ladd et al., 2005; Okkonen, 2003). Storms generated by the Aleutian Low atmospheric pressure system promote onshore advection of surface water (Cooney, 1986) and the coastal mountain range constrains these pressure systems and results in elevated precipitation and runoff (Royer, 1982). Variation in the storms and runoff result in interannual variability in the circulation and onshore advection.

To address the gauntlet hypothesis and elucidate mechanisms influencing recruitment variability for arrowtooth flounder in the GOA, we developed a spatially-explicit individual-based model (IBM) reflecting previously-known early life characteristics for arrowtooth flounder as well as important forcing mechanisms influencing the physical environment in the GOA. Spatially-explicit IBMs are biophysical models that have been used in studies of recruitment (Hinckley et al., 1996; Stockhausen and Lipcius, 2003; Kim et al., 2015), marine reserves (Stockhausen et al., 2000; Stockhausen and Lipcius, 2001; Paris et al., 2004; Stockhausen and Hermann, 2007; Pelc et al., 2010), and connectivity (Cowen et al., 2006; Cowen et al., 2007; Cooper et al., 2013), and for other applications in marine ecology and fisheries. Most commonly, the models include several pelagic early life history stages, with biological processes that differ among the stages. To simulate the environmental factors such as temperature and salinity and currents that affect development and transport of each life stage, IBMs are typically coupled to regional three-dimensional oceanographic models. IBMs used previously in recruitment and connectivity studies have ranged from quite simple with minimal mechanisms and behavior to relatively complex models that include a full suite of processes such as feeding, bioenergetics, growth and movement (e.g. Hinckley et al., 1996; Hinckley et al., 2001; Megrey and Hinckley, 2001; Werner et al., 2001; North et al., 2009; Parada et al., 2010; Kim et al., 2015). The degree of complexity often reflects the data available for a particular species as well as the research question or focus.

We used this model-based approach to explore ways in which environmental variability in the GOA may affect recruitment of arrowtooth flounder. We specifically addressed the hypothesis that *'Recruitment variability of arrowtooth flounder is primarily influenced by variability in the proportion of young fish transported from offshore spawning areas to nearshore nursery areas (connectivity) due to interannual differences in the strengths of the physical regimes that characterize the GOA environment'.* We quantified potential patterns, strengths and interannual variability of connectivity between arrowtooth flounder spawning and nursery areas over a 16-year time period (1996-2011) using a spatially-explicit IBM for arrowtooth flounder. We also explored relationships between connectivity and a suite of environmental factors to try to identify strong linkages and mechanisms driving model-derived recruitment variability. Finally, we tested a suite of potential indices from the IBM as predictors for recruitment to the population, as estimated by the 2015 stock assessment for arrowtooth flounder in the GOA (Spies et al., 2015).

2. Methods

This article is a companion paper to several others in this issue that report results from individual-based models for three of the other four focal species of the GOAIERP (i.e. Stockhausen et al., this issue; Gibson et al., this issue; Hinckley et al., this issue). In particular, the analysis undertaken in this article parallels that for Pacific ocean perch (POP) in Stockhausen et al. (this issue). To avoid extensive duplication of material in this section, where appropriate the reader will be referred to the relevant section in Stockhausen et al. (this issue) for details regarding methodology.

2.1. Modeling description

To explore connectivity between offshore spawning areas and inshore nursery areas for arrowtooth flounder in the Gulf of Alaska, we used a newly-developed, species-specific IBM coupled to a hydrodynamic model for the region. The arrowtooth flounder IBM uses daily-averaged output from a Regional Ocean Modeling System (ROMS; https://www.myroms.org/; Haidvogel et al., 2008; Shchepetkin and McWilliams, 2005) model for the coastal GOA to provide the time-varying, 3-dimensional environment for the IBM. The IBM was developed within the Dispersal Model for Early Life Stages (DisMELS) framework, a platform for creating and running IBMs based on marine fish and invertebrate species with early pelagic life stages. The IBM integrates biological processes affecting simulated individuals, including advective and diffusive movement using a Lagrangian particle tracking algorithm, as they develop in time through multiple early life stages. The reader is referred to Sections 2.1.1 and 2.1.2 in Stockhausen et al. (this issue) for general details regarding the ROMS model and the DisMELS framework.

2.1.1. IBM details

The arrowtooth flounder model is a relatively simple IBM, reflecting the limited knowledge we have for this species in its early life stages. Egg-stage development is temperature-dependent, but otherwise model processes are similar to those in the sablefish and POP IBMs (Gibson et al. and Stockhausen et al., this issue): growth rates in other life stages are stage-dependent constants and movement is essentially passive and undirected, except that individuals move vertically to remain within stage-specific "preferred" depth ranges. The arrowtooth flounder IBM consists of eight sequential early life stages, reflecting the conceptual model depicted in Fig. 1: egg, small yolk sac larva, large yolk sac larva, small feeding preflexion larva, large feeding preflexion larva, postflexion larva, settlement-stage juvenile (settler), and benthic juvenile. In the model runs for this study, life stage, age, size or egg development stage, and location (latitude, longitude, depth) were integrated on a 20 minute "biological" time step; values for *in situ* temperature and salinity were also interpolated for each individual at this time step. Information reflecting these attributes was saved for each individual at a daily time step for further analysis.

2.1.1.1. Egg stage

Blood et al. (2007) characterized 19 morphological sub-stages through which arrowtooth flounder eggs develop prior to hatching. In rearing experiments, sub-stage durations were found to be temperature dependent. These experiments were only carried out at two substantially different temperatures (rearing temperatures were 3.1, 3.2 and 6.2ºC), allowing the temperature dependence to be described by functions of two parameters, at most. To incorporate this temperature-dependence into the IBM, we modeled sub-stage-specific ln-scale development rates, $r_s(T)$, as linear functions of temperature using

$$r_s(T) = \alpha_s + \beta_s \cdot T \tag{1}$$

where *s* indicates sub-stage, *T* is temperature (in °C), and α_s and β_s are, respectively, the sub-stage-specific intercept and slope of the temperature dependence. Individual development within sub-stage s, $\Delta_s(t)$, was then given by the integral

$$\Delta_s(t) = \int_0^t \exp\left(r_s(T(t')\right) dt' \tag{2}$$

where *t* is the elapsed time since the start of the sub-stage and $T(t')$ is the *in situ* temperature experienced by the individual at t'. At constant temperature *T*, the sub-stage duration t_s was thus given by

$$\ln\left(\frac{1}{t_s}\right) = r_s(T) \tag{3}$$

We assumed the intercept parameters, α_s, were different for all sub-stages, but that the slopes of the temperature dependence were the same. Using the mean sub-stage durations from Blood et al. (2007; Fig. 2a), we thus estimated intercept parameters, α_s, for all sub-stages but only one slope parameter (i.e. $\beta_s \equiv \beta$ for every *s*). Based on our analysis, total egg stage duration is approximately three times longer at 3°C than at 7°C (~600 hrs vs. ~200 hrs; Fig. 1b).

Blood et al. (2007) noted that arrowtooth flounder eggs were seldom collected at depths less than 400 m in the GOA, and that collections of eggs at shallower depths were likely the result of transport onto the shelf by strong onshore flow and tidal mixing in deep troughs or canyons (Mordy et al., this issue). Eggs were thus assumed to be neutrally buoyant within the 300-600 m depth range (Table 1a). Simulated eggs underwent diffusive vertical random walks while within this "preferred" depth range, but rose (if deeper) or sank (if shallower) at a fixed mean ("buoyancy") rate when outside this depth range. By adjusting the relative sizes of the vertical random parameter and the buoyancy rate, it was possible to adjust how constrained simulated eggs were to the "preferred" range. Simulated eggs were also subject to diffusive horizontal random walks to incorporate sub-grid scale random motion.

2.1.2. Larval stages

Five larval stages were defined in the IBM to facilitate ontogenetic changes in "preferred" depth ranges, growth rates, and movement parameters (Tables 1a, b; Fig. 2). Simulated individuals that completed the egg stage "hatched" to become small yolk sac (SYS) larvae, at 4.4 mm SL. SYS larvae grew at a constant intrinsic rate of 0.008 day^{-1} and completed the SYS larval stage when they reached 6.1 mm SL (~41 days). The preferred depth range for SYS larvae was assumed to be the same as that for eggs, so SYS larvae nominally remained at depth (300-600 m). Outside of this preferred range, individuals would swim vertically at a mean rate of 0.1 body lengths to re-enter the preferred range. At 6.1 mm, individuals became large yolk sac (LYS) larvae and moved shallower in the water column to a preferred depth range of 150-300 m. Otherwise, LYS larvae were similar to SYS larvae. At 7.0 mm SL, after ~17 days, LYS larvae became small feeding preflexion (SFPr) larvae. Intrinsic growth rates increased to 0.01 day^{-1}, and SFPr larvae moved shallower to a preferred depth range of 40-80 m. At 10.0 mm SL (~ 36 days), SFPr larvae became large feeding preflexion (LFPr) larvae and continued their ontogenetic vertical migration to a preferred depth range of 10-30 m. Other characteristics were similar to SFPr larvae. At 13.4 mm SL (~29 days), individuals became postflexion larvae. As postflexion larvae, their horizontal diffusivity increased from 0.001 to 0.01 m^2/s (reflecting assumed increased swimming ability, but no directionality); otherwise, they were similar to LFPr larvae.

2.1.3. Juvenile stages

Two juvenile stages were defined in the IBM, the settlement-stage juvenile and the benthic juvenile (Table 1b; Fig. 2). The latter stage, however, was merely an identifier for individuals that successfully recruited to defined nursery areas: it had no dynamics. Upon reaching 42 mm SL, postflexion larvae became settlement-stage juveniles that were competent to settle to the benthos and end the sequence of early pelagic life stages. Preferred nurseries for settlement-stage juveniles were defined as areas less than 50 m deep, while areas that were 50-150 m deep were defined as alternative nurseries. Settlement-stage juveniles that reached a preferred nursery area in less than 8 days following transition from the postflexion larval stage settled to the benthos and became benthic juveniles in the nursery area; these individuals were regarded as successful recruits. At 8 days, settlement-stage juveniles that were in an alternative nursery area also settled and became benthic juveniles; these were also regarded as successful recruits. All settlement-stage individuals that did not arrive at either type of nursery habitat by the end of 8 days were considered to have died, were removed from the model, and were characterized as unsuccessful. Any individuals that did not become benthic juveniles by the end of a model run were also considered to have died and characterized as unsuccessful.

2.1.4. Initial conditions

Because the main groundfish surveys in the GOA occur in the summer on a biennial or triennial basis, there is little information on the spatial (and interannual) patterns of spawning arrowtooth flounder across the GOA to inform initial conditions in the IBM. For each model year, simulated individuals were released as stage 1 eggs ("spawned") in a series of separate "cohorts" each year at 5 m above the bottom within hypothetical "spawning areas" along the continental shelf break (see Fig. 1 in Stockhausen et al., this issue, or Fig. S1 in the Supplementary Material). Grid cells along the continental shelf edge were classified as spawning areas if the bathymetric depth at the center of the cell was between 300 and 600 m. In each cohort, individuals were released simultaneously on a 1-km *x* 1-km grid across the spawning areas, with a total 16,453 individuals in a cohort.

Observed patterns of arrowtooth flounder egg abundance in plankton sampling (Fig. 2a) indicate that the bulk of spawning activity occurs in mid-to-late January and early February. However, recent authors have hypothesized that spawning also occurs in late December/early January (e.g. Blood et al., 2007; Doyle and Mier, submitted). Consequently, we released three cohorts each year, starting on January 1 and subsequently at 15-day intervals (Fig. 2b). To incorporate the observed temporal patterns of abundance when we calculated annual connectivity for each year, we weighted individuals in the first two "cohorts" released each year by a factor of 600 (assuming the unobserved spawning in late December/early January was as intense as that observed in mid-January). Individuals in the final cohort were weighted by a factor of 480 (Fig. 2b). Possible spawning in late February and early March was ignored. Consequently, we tracked a total of 49,359 simulated individuals per model simulation.

2.2. Connectivity

As used here, "connectivity" is the probability of successful recruitment from a (offshore) spawning area to a (inshore) nursery area, where successfully-recruiting individuals are those that settle to the benthos in a nursery area and become benthic juveniles. Because we didn't include mortality processes along individual trajectories in the model runs, "connectivity" represents “maximum potential” connectivity between the spawning and nursery areas. Nursery areas that accounted for a substantial fraction of successful settlers originating from a given spawning area were considered to be “highly-connected” to that spawning area, while nursery areas that accounted for a small fraction of successful recruits were only “weakly-connected”. Using the IBM results, we quantified annual connectivity between spawning and nursery areas on alongshore scales of ~150 km using the same spatial zones and approach as used for POP (see Fig. 1 and Sections 2.2.1-2.2.3 in Stockhausen et al., this issue

2.3. Model validation and estimated recruitment

Few data exist to validate the IBM. The only suitable dataset available to compare with predictions from the IBM is the recruitment time series estimated as part of the stock assessment conducted by NOAA Fisheries (Spies et al., 2015). The stock assessment uses a statistical catch-at-age model for arrowtooth flounder in the GOA to fit fishery catch and discard information. As well, several fishery-independent datasets are used to estimate recruitment of age-1 arrowtooth flounder to the stock starting in 1961 (Fig. 23 in Spies et al., 2015) and the subsequent abundance of older age classes and spawning stock biomass. The 2015 stock assessment estimates of age-1 recruitment, lagged to the age-0 year class, are shown for 1996-2011 in Fig. 4a, along with the estimated associated spawning biomass (S). Making standard transformations to the estimated recruitment time series, such as transforming to ln-scale ($ln(R)$) or assuming a stock-recruit relationship exists ($ln(R/_S)$), had little effect on the scale of variability in recruitment after standardizing the time series (Fig. 4b). Thus, we only used the standardized recruitment time series (R, Fig. 4b) in comparisons with results from the IBM.

2.4. Analysis

Paralleling the POP analysis (Stockhausen et al., this issue), we focused analysis of the multi-year IBM results on: 1) elucidating predicted patterns of connectivity, and their variability, between large-scale spawning and nursery zones and 2) testing whether variability in recruitment to the GOA arrowtooth flounder stock (as estimated in its stock assessment) appeared to be reflected in the connectivity indices derived from the IBM.

2.4.1. Connectivity matrices

We characterized long-term connectivity between the large-scale spawning and nursery zones using the temporal median of the annual connectivity matrices, $\tilde{C}_{n,s}$, as well as overall temporal variability in connectivity by calculating the temporal root median square deviation (see Fig. 1 and Section 2.4.1.1 in Stockhausen et al., this issue). To better elucidate spatial and temporal patterns of variability in connectivity, we decomposed the time series of annual connectivity matrices, $C_{n,s}(y)$, into a set of orthogonal spatial loadings and temporal principal component scores using empirical orthogonal function (EOF) analysis (Preisendorfer, 1988; see Section 2.4.1.2 in Stockhausen et al., this issue, for details).

2.4.2. Environmental indices potentially associated with aggregate connectivity indices

Using a multivariate, multispecies hierarchical Bayesian approach and much longer time series, Stachura et al. (2014) found that recruitment in the GOA for a “cross-shelf transport” group (of which arrowtooth flounder was a member) was “strongly” related to the first two principal components of sea surface height (SSH) variability in the GOA. The first PC was related to onshore Ekman transport, coastal downwelling, and an accelerated Alaska Coastal

Current, as well as both the El Nino-Southern Oscillation (ENSO) and the Pacific Decadal Oscillation (PDO). As such, we hypothesized that variability in large-scale environmental indices such as the Arctic Oscillation (AO), the Multivariate ENSO Index (MEI), and the PDO, or regional-scale indices for cross-shelf flow (developed directly from the ROMS model) might be strongly reflected in variability in connectivity. Because arrowtooth flounder spawning occurs during the winter, we added winter-averaged time series for the AO, MEI, PDO, and the ROMS-derived cross-shelf flow to those used in the POP analysis (as described in Section 2.4.2 in Stockhausen et al., this issue; see also Table 2 here and Fig. S2 in the Supplementary Material).

As with POP, we limited our analysis to the aggregate connectivity indices reflecting total settlement success by spawning zone (i.e. the $C_s(y)$), as well as the time series of scores from the first two principal components in the EOF analysis, and tested the environmental indices as potential predictors of the aggregate connectivity indices using simple linear models (for details, see Section 2.4.2 in Stockhausen et al., this issue).

2.4.3. Connectivity and recruitment

Finally, we tested the aggregate connectivity indices as potential predictors for recruitment using simple linear models of the form $\tilde{R}(y) = \sum_i \beta_i \cdot \tilde{I}_i(y)$ where $\tilde{R}(y)$ denotes the standardized (as z-scores) annual recruitment time series from the 2015 GOA arrowtooth flounder stock assessment model (Spies et al., 2015), β_i is the *i*th regression parameter, and $\tilde{I}_i(y)$ denotes the standardized time series for the *i*th aggregate index. We tested all models with six spawning zones or fewer using the R package “glmulti” (Calcagno and de Mazancourt, 2010; R Core Team, 2015) and used AICc (Burnham and Anderson, 2002) to select the “best” one. The estimated β_is from the best model should reflect the spatial pattern of spawning if variability in recruitment really is driven by variability in connectivity and if the spatial pattern of spawning was relatively constant during 1996-2011.

3. Results

3.1 IBM output

As noted previously, individuals were released on a 1-km *x* 1-km grid across spawning areas defined as ROMS grid cells with bathymetric depths between 300 and 600 m, with a total of 16,453 individuals per released cohort. Because actual release depths on the 1-km *x* 1-km grid were interpolated within each ROMS grid cell classified, individual release depths spanned a somewhat wider range than 300-600 m (see Fig. S3 in the Supplementary Material). About 11% of simulated eggs were released outside this nominal interval.

Most simulated individuals exhibited a general trend to move to the north and west during the simulations, but individual trajectories were complex—indicating the influence of mesoscale and larger eddies on their movement (e.g. Fig. 3). Most individuals remained off the shelf in deeper water until reaching at least the small feeding preflexion (SFPr) larval stage, at which point they moved up in the water column (nominally 40-80 m depth). Many individuals that were not successful in recruiting to suitable nursery habitat during the allotted time frame were transported farther off shelf (away from nursery habitats) into the deep ocean zone *vis-a-vis* most "successful" individuals. Successful individuals tended to stay on the shelf, although a fair number were also transported off the shelf only to return via eddies and gyres. While a few individuals that were spawned in the southeast (zones 1-3) exited the model grid at its southeast boundary, many more exited the grid at its western boundary due to the general counter-clockwise nature of the mean circulation along the shelf.

Individuals that exited the grid were classified as unsuccessful. As a result of the general circulation pattern, and because of its proximity to the western boundary of the model grid, no individuals spawned in zone 12 (Shumagin Islands) were successful in any model year (Fig. 4a). Simulated individuals spawned in the eastern half of the GOA (zones 1-5) were more likely (~10-40%) to reach nurseries in the allotted time than those spawned in the western half (zones 7-12; 0-5%). Interannual variability in the fraction successful from any spawning zone was large relative to the mean. Most successful individuals moved to nurseries north and west of the zone in which they were spawned (Fig. 4b).

3.2. Connectivity matrices

3.2.1. Long-term patterns

The cell-by-cell median and root median square deviation of the annual connectivity matrices (Fig. 5) indicate that the highest median connectivity between spawning and nursery areas was between spawning in zones 2 and 3 (Sitka and Cross Sound) and nurseries in zone 6 (PWS). Median connectivity was directed in a counterclockwise fashion, with spawning in the south and east (lower number alongshore zones) connected with nurseries to the north and west (higher number alongshore zones). While some retention occurred for spawning in the east (zones 1-6), the level was generally quite small (< 0.5%) although retention in zone 2 (Sitka) reached 1.4%. For spawning in the west (zones 7-12), median retention was essentially zero. Median connectivity from west to east (clockwise transport) was negligible, even for adjacent zones, although it occurred in rare circumstances (Fig. S4 in the Supplementary Material). Temporal variability was positively correlated with median connectivity, so the most highly-connected cells also tended to display the highest variability (Fig. 7b).

The highest fraction of individuals recruiting from spawning in zone *s* to nurseries in zone *n* was 18.0% in 2001 for 3→6 (Cross Sound to PWS; Fig. S4 in the Supplementary Material). In fact, this pathway accounted for five of the six highest connectivity values over all 16 simulated years. The other pathway that accounted for the top value in more than one year was 2→6 (Sitka to PWS; six years). PWS (zone 6) constituted the most highly connected nursery zone in all but two years. Thus, the most highly connected spawning zones were separated approximately 650 km (3: Cross Sound) and 800 km (2: Sitka) from the most highly-connected nursery zone (6: PWS).

3.2.2. EOF analysis

The first two EOFs of the annual connectivity matrices accounted for ~63% of the total variance, with much smaller contributions from additional components (Fig. S6 in the Supplementary Material). Positive principal component scores on the first EOF (Fig. 8) were associated with higher connectivity between spawning zones 3 and 4 (Cross Sound and Yakutat) and nurseries in zone 6 (PWS) and between spawning zones 5 and 6 (Icy Bay and PWS) and nurseries in zones 7 and 8 (Kenai and North Kodiak). Positive scores on the first EOF were also associated with reduced connectivity between spawning in the far east (alongshore zones 1 and 2; PWI and Sitka) and nurseries west of Icy Bay (i.e. zones > 5). Positive principal component scores on the second EOF primarily reflected higher connectivity between spawning zones 1, 2 and 3 (PWI, Sitka and Cross Sound) and nurseries in zone 6 (PWS).

3.3. Aggregate connectivity indices

3.3.1. Time series

Time series for the aggregate annual connectivity indices $C_s(y)$, the total fraction of successful individuals spawned in alongshore zone s, indicated substantial temporal variation in settlement success for individual zones, as well as regional differences (Fig. 9). Mean settlement success, and variability, was highest for the eastern zones (1-6), while it was sporadic (at best) for the western zones (7-12). 2007 stood out slightly among the zones in the eastern region as the year in which the highest fraction of successful settlers occurred for any spawning zone (almost 50% from zone 3, Cross Sound), while in the western region 2009 stood out as the year in which relatively high success (~15%) occurred for several spawning zones (7 and 8, Kenai and North Kodiak).

3.3.2. Linear model analysis for environmental indices potentially associated with connectivity

We found relatively weak evidence (Table 3) for relationships between the aggregate connectivity indices and any of the 24 large- (AO, MEI, PDO) or regional-scale (ROMS-derived cross-shelf flow) environmental indices we considered as potentially-explanatory drivers. The "best" models, using AICc as the selection criterion, for the $C_s(y)$ from six alongshore zones (1, 6, 7, 8, 9 and 10) yielded adjusted R^2 values of 50% or better. However, when adjusted for multiple comparisons using a bootstrapping approach to evaluate model significance, the models for zones 1, 6 and 7 were not significant and the remaining three were only marginally significant with empirical p-values of 0.05-0.07. The combination of the spring MEI and spring PDO indices was selected as the best 2-covariate model for three of the six zones (7, 8, and 9) where the adjusted R^2 was greater than 0.5. For these models, the regression coefficient for the spring MEI was always positive while that for the spring PDO was negative.

3.4. Connectivity and recruitment

3.4.1. Time series

Estimated recruitment from the 2015 GOA arrowtooth flounder stock assessment (Spies et al., 2015) exhibited decadal scale fluctuations about a long-term mean of ~10^9 individuals during years for which the IBM was run, with peaks in 1999 and 2011 and a low in 2009 (Fig. 4a). In contrast, estimated spawning biomass was relatively constant at ~870,000 t between 1996 and 2005, after which it slowly increased to ~1,150,000 t in 2011 (Fig. 4a).

3.4.2. Linear model analysis for aggregate connectivity indices as predictors of recruitment

Although we tested all linear models for recruitment containing aggregate connectivity indices from up to six spawning zones as potential covariates (over 2,500 models), none of these explained recruitment variability better than the mean (using AICc as the model selection criterion).

4. Discussion

The guiding hypothesis of the GOAIERP program was that successful recruitment of arrowtooth flounder (and the other four focal species) in the GOA is primarily determined by processes which occur during the larval and early juvenile stages, in the "gauntlet" between spawning in offshore natal areas and settlement in nearshore nurseries as young-of-the-year. Of the many interrelated processes that can occur during this time period, this study focused on whether or not variability in transport mechanisms, as reflected in variability in connectivity between offshore natal zones and inshore nursery habitats, could account for subsequent variability in recruitment of arrowtooth flounder as estimated by a stock assessment model (Spies et al., 2015). We used linked models, specifically, a regional oceanographic model, and a species-specific, Lagrangian IBM to address this issue.

The arrowtooth flounder IBM described here was an attempt to combine current knowledge regarding early-life processes at the individual and population-level (e.g. seasonality of spawning, temperature-dependent egg development, larval growth) with ecosystem-level mechanisms (e.g. current patterns) in a synthetic fashion across spatiotemporal scales from centimeters and minutes to 100s of kilometers and months-to-years in order to assess the extent to which variability in passive physical transport from offshore spawning areas to nearshore juvenile nurseries could account for subsequent variability in recruitment to the population. Because we lacked information on variability in mortality processes along individual trajectories, we focused our analysis of results from the IBM on estimating "maximum potential" connectivity between potential offshore spawning areas and nearshore nursery habitats using alongshore spatial scales on the order of 150 km. Although "maximum potential" connectivity does not include mortality processes acting along individual pathways, it does incorporate variability in transport processes and seasonality in spawning. Estimates of even such a narrowly-defined version of connectivity may generate hypotheses regarding the fate of individual fish spawned in particular regions, the potential importance of different spawning and nursery areas, and the impacts of larger scale climate forcing on these patterns. Lagrangian IBMs are one of the few available tools for predicting connectivity, because of their ability to follow simulated individuals along transport pathways.

4.1. Individual pathways

Results from the IBM suggest that, as young arrowtooth flounder progress through early pelagic life stages from egg to newly-settled, young-of-the-year benthic juvenile, there is a predominant pattern of counter-clockwise (southeast to northwest) dispersal along the continental shelf, as successfully-settling individuals are transported from deeper spawning areas along the shelf break to shallower, inshore nursery areas (e.g. Figs. 5 and 6b). Individual pathways are complex—indicating the influence of mesoscale and larger eddies on their movement. While many individuals are transported away from the shelf, some of these are eventually transported back onto the shelf (a few even after ending up several hundred km offshore). Typical alongshore dispersal distances from spawning to nursery areas were on the order of several hundred km, while the potential for retention or clockwise movement was quite small. Most individuals (typically >80%) in the model runs were not successful in reaching inshore nursery habitat from offshore spawning areas. Many of these “unsuccessful” individuals were transported beyond the modeled area, particularly to the northwest, suggesting the western

GOA population may provide recruits to populations in the Aleutian Islands or the eastern Bering Sea.

The envelopes of the "late stage" larval trajectories illustrated in Fig. 5 are fairly similar to those obtained for POP (Fig. 5 in Stockhausen et al., this issue), which is not surprising given that these stages are in the water column at roughly the same time for both species as well as the similarity of modeled movement behavior for these stages in both models. As with POP, the convoluted nature of many of the trajectories illustrated in Fig. 5 has strong implications for larval surveys conducted in the GOA, particularly with reference to the inherent uncertainty regarding the origin or destination of individuals collected during such cruises.

4.2. Connectivity

The highest fraction of individuals that successfully settled in inshore nursery areas originated from areas in the eastern GOA, while the nursery areas to which those individuals dispersed were in the central and western GOA. This east-to-west connection between putative spawning and nursery areas reflects the general circulation patterns in the GOA, which are dominated by the counter-clockwise circulation of the Alaska Gyre (Alaskan Stream/Alaska Current system) over the shelf break (Reed, 1984) and the buoyancy-driven Alaska Coastal Current on the shelf (Royer, 1998; Stabeno et al., 2004). The GOA has multiple hydrographic fronts which can hinder on-shelf transport (Belkin et al., 2002; 2003). However, this region is generally thought of as being a downwelling shelf because of the onshore Ekman transport that results from storms generated by the Aleutian Low Pressure system (Weingartner et al., 2005). Previous observations have implicated the wind generated Ekman transport in the advection of

oceanic zooplankton onto the shelf (Cooney, 1986). Here we have shown that there is sufficient on-shelf advection to transport young arrowtooth flounder from off-shelf deep spawning sites to shallow onshore nursery areas, without the inclusion of any directed horizontal swimming behavior, e.g. towards shallower bathymetry, food, or a particular geographic location.
The east-west connection is also reflected in the spatial pattern of arrowtooth flounder biomass in biennial fishery-independent trawl surveys conducted by the Alaska Fisheries Science Center. In the 2013 summer bottom trawl survey, the southeastern Alaska and Yakutat survey strata (alongshore zones 1-6, roughly speaking) accounted for ~63% of presumed arrowtooth flounder spawning biomass (i.e. in depths greater than 300 m), whereas the Shumagin, Chirikof, and Kodiak strata (roughly alongshore zones 7-12) accounted for ~72% of presumed juvenile biomass (i.e. in depths shallower than 300 m). Our results, as well as the spatial pattern of abundance from the trawl survey, suggest that juvenile arrowtooth flounder in the western GOA must undergo a contranatant alongshore migration from west-to-east (as well as an offshore movement to deeper water) to maintain spawning stock biomass in the eastern GOA if the stock can be regarded as a closed population.

4.3. Environmental indices potentially associated with connectivity

As noted in Section 2.4.2, Stachura et al. (2014) found that recruitment in the GOA for a “cross-shelf transport” group (of which arrowtooth flounder was a member) was “strongly” related to the first two principal components of sea surface height (SSH) variability in the GOA. The first PC was related to onshore Ekman transport, coastal downwelling, and an accelerated Alaska Coastal Current, as well as both ENSO and the PDO. As such, we hypothesized that variability in large-scale environmental indices such as the AO, MEI and PDO or regional-scale indices for cross-shelf flow developed directly from the ROMS model might be strongly reflected in variability in connectivity.

Instead, we found that variability in aggregate connectivity was generally poorly predicted by the large- and regional-scale indices we tested (Table 3). Thus, it appears that variability in IBM-derived connectivity is not simply related to spatiotemporal averages of quantities reflecting physical forcing mechanisms. Considering the dynamic nature of current patterns in the GOA and the resultant complexity of the some of the pathways individuals took in the IBM, it is not surprising that indices based on an Eulerian perspective (the large-scale environmental and ROMS cross-shelf flow indices) would not capture what are inherently Lagrangian processes involving fairly large spatial (100s of km) and temporal (months) scales.

Somewhat intriguingly, though, we did find that using the springtime averages of the MEI and PDO as covariates resulted in the linear models that best described variability in aggregate connectivity for three of the alongshore zones (7, 8 and 9; Kenai, North Kodiak and South Kodiak; Table 3). While the adjusted R^2 for these models ranged from 56% to 70%, reflecting reasonably good fits, only one model (zone 9) was statistically significant after adjusting for multiple comparisons (hence our conclusions above). Although the springtime MEI and PDO were somewhat positively correlated during the 1996-2011 time period (R^2=20%), the regression coefficients for the two covariates were of opposite signs (MEI > 0, PDO < 0) in the models for each zone. Because positive anomalies in the PDO are generally associated with stronger downwelling and increased precipitation in the GOA, and consequently faster current speeds in the Alaska Coastal Current (Mantua et al., 1997; Royer, 2005), this implies individuals spawned in the western GOA may be more likely to be exported from the GOA to the Aleutian

Islands or the eastern Bering Sea during years when the springtime PDO is large. However, without extending the model time frame to increase sample sizes, our results are merely suggestive at best.

4.4. Predicting recruitment

Identifying indices that explain 50% or more of the variability in recruitment may improve recruitment estimates from stock assessment models (De Olivera and Butterworth, 2005). Here, we tested combinations of the time series of the aggregated connectivity indices as potential linear predictors for arrowtooth flounder recruitment variability (as estimated in the most recent stock assessment, Spies et al., 2015). Of the ~2,500 possible models we evaluated, the "best" model for recruitment was one in which none of the connectivity indices were included.

Thus, variability in recruitment of age 1 arrowtooth flounder in the GOA appears to be driven by more than just variability in "maximum potential" connectivity. This suggests that, like POP (Stockhausen et al., this issue), environmentally-mediated changes in mortality and growth along the trajectories of "successful" individuals substantially alter the patterns of "effective" connectivity, obtained by including these biological processes, from those of "maximum potential" connectivity obtained by considering only physical (transport) processes.

4.5. Further considerations

The failure to adequately predict recruitment does not negate the value of the IBM, nor of this study. Although one can hope for more, models should generally be expected to be only as good as the data and observations on which they are based. In this study, we hypothesized that variability in maximum potential connectivity (i.e. transport) between offshore spawning and inshore nursery areas was the main factor driving juvenile recruitment variability as estimated by the stock assessment model (Spies et al., 2015). Our results suggest little predictive power, at best, for age-1 recruitment to the population using the suite of IBM-related indices we tested.

However, it is premature to reject the hypothesis regarding the relative importance of connectivity on recruitment. There are a number of obvious factors which could contribute to the disconnect between the IBM connectivity-based results and recruitment. One factor is that spawning may vary spatially on an interannual basis in a manner that is not currently captured in the IBM, in which we have assumed that the density of egg production is uniform across the GOA in the 300-600 m bathymetric depth range. The models we considered based on the aggregate connectivity indices from the IBM presume that the relative weights among the alongshore spawning areas are fixed across time, so that substantial interannual variability in the relative importance of these areas would degrade any relationship between the indices and recruitment.

Another factor is that we may not have correctly captured the real-world processes affecting connectivity in the IBM. The ROMS model we used to provide the environment experienced by simulated individuals in the IBM has been show to capture important features of the circulation in the GOA and to be a reasonably good representation of the variability of oceanographic processes on seasonal time scales (Hermann et al., 2009a; Hermann et al., 2009b; Hermann et al., 2016). However, because the CGOA ROMS model does not incorporate data assimilation, features such as mesoscale eddies are well-represented in the model only in a statistical sense, and individual eddies in the GOA at place *x* and time *y* are not necessarily reproduced in the ROMS model output. The degree to which this mismatch affects the IBM results is unclear, but given that the IBM is based on Lagrangian integration and "following the flow", even small differences between model and reality may easily lead to large effects on individual trajectories.

Additionally, the biological processes captured in the IBM include only extremely simple characterizations of behavior (e.g. undirected swimming) and larval growth (constant growth rates), and we ignored mortality. Potential improvements to the IBM might include directed swimming, environmentally-sensitive growth rates, and size-specific mortality. Directed swimming behavior could substantially reduce alongshore dispersion or facilitate transport to particular nursery areas. Environmentally-sensitive growth rates could reduce or prolong life stage durations, altering both the timing when pelagic larvae become competent to settle to the benthos and survival rates, thus altering connectivity.

The last possibility, of course, is that the hypothesis is wrong and that variability in connectivity is not the major factor in determining recruitment strength at age 1. Even if this is indeed the case, the IBM could still be used to address the importance of variability in transport *per se* relative to environmental variability (e.g. temperature) affecting growth or survival along individual trajectories. Unfortunately, we do not currently have data to inform more sophisticated models, e.g. incorporating temperature-dependent growth or bioenergetics.

5. Conclusions

Our major findings in this study were that: 1) there is sufficient on-shelf advection to transport young arrowtooth flounder from off-shelf spawning sites to on-shelf nursery areas without active movement, 2) >80% of individuals were unsuccessful in dispersing from presumed spawning areas along continental shelf break to inshore nurseries, 3) young arrowtooth flounder settling in nursery areas throughout the GOA are likely spawned in the eastern to central GOA, and 4) arrowtooth flounder spawning in the western GOA likely contribute little to the population in the GOA (but may to populations in the Aleutian Islands or eastern Bering Sea). We also found that IBM-derived connectivity indices were not simple functions of either large-scale environmental or regional-scale cross shelf flow indices, and that the current IBM is an inadequate predictor of variability in recruitment from the stock assessment model and cannot, at this point, provide a suitable predictive index of recruitment to improve the assessment model.

Acknowledgments

This work was funded by the North Pacific Research Board (NPRB)-sponsored Gulf of Alaska Integrated Ecosystem Research Program (GOAIERP) under award #G84. This work was also supported in part by a grant of High Performance Computing resources from the Arctic Region Supercomputing Center. This manuscript is NPRB publication number 670, GOAIERP publication number 28, contribution EcoFOCI-0860 to NOAA's Fisheries-Oceanography Coordinated Investigations, Pacific Marine Environmental Laboratory contribution number 4433, and Alaska Fisheries Science Center publication number 2898. This publication is partially funded by the Joint Institute for the Study of the Atmosphere and Ocean (JISAO) under NOAA Cooperative Agreement NA15OAR4320063, Contribution No.2018-0145. The authors would like to thank K. Hedstrom for her effort in the initial development of the ROMS coastal Gulf of Alaska model on which our experiments were based, as well as A. Punt for his contributions as NPRB's Modeling Coordinator. We would also like to thank K. Shotwell and three anonymous reviewers for their comments and suggestions on the original draft of this paper.

The findings and conclusions in the paper are those of the author(s) and do not necessarily represent the views of the National Marine Fisheries Service. Reference to trade names does not imply endorsement by the National Marine Fisheries Service, NOAA.

References

Aydin, K., Gaichas, S., Ortiz, I., Kinzey, D., Friday, N., 2007. A comparison of the Bering Sea, Gulf of Alaska, and Aleutian Islands large marine ecosystems through food web modeling. U.S. Dep. Commer. NOAA Tech. Memo. NMFS-AFSC178. 298 pp.

Bailey, K.M., Picquelle, S., 2002. Larval distribution of offshore spawning flatfish in the Gulf of Alaska: potential transport pathways and enhanced onshore transport during ENSO events. Mar. Ecol. Prog. Ser. 236: 205-217.

Bailey, K.M., Stabeno, P.J., Powers, D.A., 1997. The role of larval retention and transport features in mortality and potential gene flow of walleye pollock. J. Fish Biol. 51, 135-154.

Belkin, I.M., Krishfield, R., Honjo, S., 2002. Decadal variability of the North Pacific Polar Front: Subsurface warming versus surface cooling. Geophys. Res. Lett. 29. doi:10.1029/2001GL013806.

Belkin, I.M., Cornillon, P., Ullman, D., 2003. Ocean fronts around Alaska from satellite SST data. In: Proceedings of the American Meteorological Society 7th Conference on Polar Meteorology and Oceanography. Hyannis, MA. Paper 12.7. 15pp.

Blood, D.M., Matarese, A.C., Busby, M.S., 2007. Spawning, egg development, and early life history dynamics of arrowtooth flounder (*Atheresthes stomias*) in the Gulf of Alaska. U.S. Dep. Commer., NOAA Professional Paper NMFS 7. 28 pp.

Bouwens, K.A., Smith, R.L., Paul, A.J., Rugen, W., 1999. Length at and timing of hatching and settlement for arrowtooth flounders in the Gulf of Alaska. Alaska Fish. Res. Bull. 6,41-48.

Burnham, K. P.; Anderson, D.R., 2002. Model Selection and Multimodel Inference: A Practical Information-Theoretic Approach, second edition. Springer-Verlag, New York.

Calcagno, V., C. de Mazancourt, C., 2010. glmulti: An R Package for Easy Automated Model Selection with (Generalized) Linear Models. J. Stat. Soft. 34.12, 1-29.

Cooney, R.T., 1986. The seasonal occurrence of *Neocalanus cristatus*, *Neocalanus plumchrus*, and *Eucalanus bungii* over the shelf of the northern GOA. Cont. Shelf Res. 5, 541–553. https://doi.org/10.1016/0278-4343(86)90075-0

Cooper, D.W., Duffy-Anderson, J.T., Stockhausen, W.T., Cheng, W., 2013. Modeled connectivity between northern rock sole (*Lepidopsetta polyxystra*) spawning and nursery areas in the eastern Bering Sea. J. Sea Res. 84, 2-12. https://doi.org/10.1016/j.seares.2012.07.001

Cowen, R.K., Paris, C.B., Srinivasan, A., 2006. Scaling of Connectivity in Marine Populations. Science 311, 522-527.

Cowen, R.K., Gawarkiewicz, G., Pineda, J., Thorrold, S.R., Werner, F.E., 2007. Connectivity in Marine Systems: An Overview. Oceanogr. 20(3), 14-21.

De Olivera, J.A.A., Butterworth, D.S., 2005. Limits to the use of environmental indices to reduce risk and/or increase yield in the South African anchovy fishery. Afr. J. Mar. Sci. 27, 191-203.

Doyle, M.J., Mier, K.L., 2016. Early life history pelagic exposure profiles of selected commercially important fish species in the Gulf of Alaska. Deep Sea Res. II 132, 162-93. https://doi.org/10.1016/j.dsr2.2015.06.019

Gibson, G.A., Stockhausen, W. Coyle, K.O., Hinckley, S., Parada, C., Hermann, A., Doyle, M., Ladd, C, this volume. An individual-based model for Sablefish: Exploring the connectivity between potential spawning and nursery grounds in the Gulf of Alaska. Deep Sea Res. II.

Haidvogel, D.B., and co-authors, 2008. Regional Ocean Forecasting in Terrain-following Coordinates: Model Formulation and Skill Assessment. J. Comput. Phys. 227, 3595-3624.

Hermann, A.J., Curchitser, E.N., Haidvogel , D.B., Dobbins, E.L., 2009a. A comparison of remote versus local influence of El Nino on the coastal circulation of the Northeast Pacific. Deep Sea Res. II 56, 2427-2443. https://doi.org/10.1016/j.dsr2.2009.02.005

Hermann, A.J., Hinckley, S., Dobbins, E.L., Haidvogel, D.B., Bond, N.A., Mordy, C., Kachel, N., Stabeno, P.J., 2009b. Quantifying cross-shelf and vertical nutrient flux in the GOA with a spatially nested, coupled biophysical model. Deep Sea Res. II 56, 2474-2486. https://doi.org/10.1016/j.dsr2.2009.02.008

Hermann, A.J., Ladd, C., Cheng, W., Curchitser, E., Hedstrom, K., 2016. A model-based examination of multivariate physical modes in the GOA. Deep Sea Res. II 132, 68-89. https://doi.org/10.1016/j.dsr2.2016.04.005

Hinckley, S., A.J. Hermann and B.A. Megrey, B.A., 1996. Development of a spatially-explicit, individual-based model of marine fish early life history. Mar. Ecol. Prog. Ser. 139:47-68.

Hinckley, S., Hermann, A.J., Mier, K.L., Megrey, B.A., 2001. Importance of spawning location and timing to successful transport to nursery areas: a simulation study of GOA walleye pollock. ICES J. of Mar. Sci. 58, 1042–1052.

Hinckley, S., Coyle, K.O., Gibson, G., Hermann, A.J., Dobbins, E.L., 2009. A biophysical NPZ model with iron for the GOA: Reproducing the differences between an oceanic HNLC ecosystem and a classical northern temperate shelf ecosystem. Deep Sea Res. II 56, 2520-2536. https://doi.org/10.1016/j.dsr2.2009.03.003

Hinckley, S., Stockhausen, W., Coyle, K.O., Laurel, B., Gibson, G.A., Parada, C., Hermann, A., Doyle, M., Hurst, T., this volume. Connectivity between spawning and nursery areas for Pacific cod (*Gadus macrocephalus*) in the Gulf of Alaska. Deep Sea Res. II.

Hirschberger, W.C., and G.B. Smith.1983. Spawning of twelve groundfish species in the Alaska and Pacific coast regions, 1975–1981. U.S. Dept. Commer., NOAA Tech. Memo. NMFS F/NWC-44, 50 p.

Janout, M.A., Weingartner, T.J., Okkonen, S.R., Whitledge, T.E., Musgrav, D.L., 2009. Some characteristics of Yakutat Eddies propagating along the continental slope of the northern GOA. Deep Sea Res. II 56, 2444–2459. https://doi.org/10.1016/j.dsr2.2009.02.006

Johnson, S.L., Quinn, T.J., 1988. Catch-age analysis with auxiliary information of sablefish in the Gulf of Alaska. Alaska Center for Fisheries and Ocean Sciences, University of Alaska, Juneau, Alaska. . 79 pp.

Kim, J.J., Stockhausen, W., Kim, S., Cho, Y.-K., Seo, G.-H., Lee, J.-S., 2015. Understanding interannual variability in the distribution of, and transport processes affecting, the early life stages of *Todarodes pacificus* using behavioral-hydrodynamic modeling approaches. Prog. Ocean. 138, 571-583. https://doi.org/10.1016/j.pocean.2015.04.003

Ladd, C., Stabeno, P., Cokelet, E.D., 2005. A note on cross-shelf exchange in the northern GOA. Deep Sea Res. II 52, 667–679. https://doi.org/10.1016/j.dsr2.2004.12.022

Ladd, C., Stabeno, P.J., 2009. Freshwater transport from the Pacific to the Bering Sea through Amukta Pass. Geophys. Res. Lett. 36, L14608. https://doi.org/10.1029/2009GL039095

Mantua, N.J., Hare, S.R., Zhang, Y., Wallace, J.M., Francis, R.C., 1997. A Pacific interdecadal climate oscillation with impacts on salmon production. Bull. Am. Met. Soc. 78, 1069-

1079.

Matarese, A.C., Blood, D.M., Picquelle, S.J., Benson, J.L., 2003. Atlas of abundance and distribution patterns of ichthyoplankton from the Northeast Pacific Ocean and Bering Sea ecosystems based on research conducted by the Alaska Fisheries Science Center (1972-1996). U.S. Dep. Commer., NOAA Professional Paper, NMFS-1. 281 pp.

Matarese, A.C., Kendall, A.W., Blood, D.M., Vinter, B.M., 1989. Laboratory Guide to Early Life Stages of Northeast Pacific Fishes. U.S. Dep. Commer., NOAA Technical Report NMFS 80. 652 pp.

Megrey, B.A., Hinckley, S., 2001. The effect of turbulence on feeding of larval fishes: a sensitivity analysis using an individual-based model. ICES J. Mar. Sci. 58, 1015-1029.

Mordy, C.W., Stabeno, P.J., Kachel, N.B., Kachel, D., Ladd, C., Zimmerman, M., Doyle, M., this issue. Importance of canyons to the northern Gulf of Alaska ecosystem. Deep Sea Res. II.

North, E.W., Gallego, A., Petitgas, P., 2009. Manual of recommended practices for modelling physical-biological interactions during fish early life. ICES Coop. Res. Rep. No. 295.

Okkonen, S.R., 2003. Satellite and hydrographic observations of eddy-induced shelf-slope exchange in the northwestern GOA. J. Geophys. Res. 108, 3033. https://doi.org/10.1029/2002JC001342

Parada, C., Armstrong, D.A., Ernst, B., Hinckley, S., Orensanz, J.M., 2010. Spatial dynamics of snow crab (*Chionoecetes opilio*) in the eastern Bering Sea—putting together the pieces of the puzzle. Bull. Mar. Sci. 86, 413-437.

Paris, C.B., K.C. Lindeman, R. Claro, J.L. Fortuna, and R.K. Cowen K. 2004. Modeling Larval Transport from Snapper (*Lutjanidae*) Spawning Aggregations in Cuba. Proc. Gulf Caribb. Fish. Inst. 55, 570-576.

Pelc, R.A.; Warner, R.R., Gaines, S.D., Paris, C.B., 2010. Detecting larval export from marine reserves. Proc. Nat. Acad. of Sci. 107.43 (Oct 26, 2010), 18266-18271.

Preisendorfer, R.W., 1988. Principal Component Analysis in Meteorology and Oceanography. Elsevier Press. 425 pp.

R Core Team, 2015. R: A language and environment for statistical computing. R Foundation for Statistical Computing, Vienna, Austria. http://www.R-project.org/

Reed, R.K., 1984. Flow of the Alaskan Stream and its variations. Deep Sea Res. 31, 369–386.

Reed, R.K., Schumacher, J.D., 1984. Additional current measurements in the Alaskan Stream near Kodiak Island. J. Phys. Oceanogr. 14, 1239-1246.

Rickey, M.H., 1995. Maturity, spawning, and seasonal movement of arrowtooth flounder off Washington. Fish. Bull. 93,127-138.

Royer, T.C., 1982. Coastal freshwater discharge in the northeast Pacific. J. Geophys. Res. 87(C3), 2017-2021.

Royer, T. 1998. Coastal Processes in the Northern North Pacific. In: Brink, K.H., Robinson, A.R. (Ed.s), The Sea, Vol. 11. John Wiley & Sons, New York, p. 395-414.

Royer, T.C., 2005. Hydrographic responses at a coastal site in the northern Gulf of Alaska to seasonal and interannual forcing. Deep Sea Res. II. 52, 267–288.

Shchepetkin, A.F., McWilliams, J.C., 2005. The regional oceanic modeling system (ROMS): a split-explicit, free-surface, topography-following-coordinate oceanic model, Ocean Model. 9(4), 347-404.

Spies, I., Ianelli, J.N., Kingham, A., Narita, R.,Palsson, W. 2015. 7. Assessment of the arrowtooth flounder stock in the Gulf of Alaska. In: Appendix B: Stock Assessment and

Fishery Evaluation Report for the Groundfish Resources of the Gulf of Alaska. North Pacific Fishery Management Council, 605 W 4th Avenue, Suite 306, Anchorage, AK 99501. https://www.afsc.noaa.gov/REFM/Docs/2015/GOAatf.pdf

Stabeno, P.J., N.A. Bond, N.A., Hermann, A.J., Kachel, N.B., Mordy, C.W., Overland, J.E., 2004. Meteorology and oceanography of the northern GOA. Cont. Shelf Res. 24, 859–897.

Stabeno, P.J., Bell, S., Cheng, W., Danielson, S., Kachel, N.B., Mordy, C.W., 2015a. Long-term observations of Alaska Coastal Current in the northern Gulf of Alaska. Deep Sea Res. II 132, 24-40. https://doi.org/10.1016/j.dsr2.2015.12.016

Stabeno, P.J., Bond, N.A., Kachel, N.B., Ladd, C., Mordy, C., Strom, S.L., 2015b. Southeast Alaskan shelf from southern tip of Baranof Island to Kayak Island: Currents, mixing and chlorophyll-a. Deep Sea Res. II 132, 6-23. https://doi.org/10.1016/j.dsr2.2015.06.018

Stachura, M.M., Essington, T.E., Mantua, N.J., Hollowed, A.B., Haltuch, M.A., Spencer, P.D., Branch, T.A., Doyle, M.J., 2014. Linking Northeast Pacific recruitment synchrony to environmental variability. Fish. Oceanogr. 23, 389-408.

Stockhausen, W., Hermann, A., 2007. Modeling larval dispersion of rockfish: A tool for marine reserve design? In: Heifetz, J., DiCosimo, J., Gharrett, A.J., Love, M.S., O'Connell, T., Stanley, R. (Eds.), Biology, assessment, and management of North Pacific rockfishes. Alaska Sea Grant College Program, University of Alaska Fairbanks. p. 251-274.

Stockhausen, W., Lipcius, R., 2001. Single large or several small marine reserves for the Caribbean spiny lobster? Mar. Freshw. Res. 50, 1605-1614.

Stockhausen, W., Lipcius, R., 2003. Simulated effects of seagrass loss and restoration on settlement and recruitment of blue crab postlarvae and juveniles in the York River, Chesapeake Bay. Bull. Mar. Sci. 72, 409-422.

Stockhausen, W., Lipcius, R., Hickey, B., 2000. Joint effects of larval dispersal, population regulation, marine reserve design and exploitation on production and recruitment in the Caribbean spiny lobster. Bull. Mar. Sci.. 66, 957-990.

Stockhausen, W.T., Coyle, K.O., Hermann, A.J., Doyle, M., Gibson, G.A., Hinckley, S., Ladd, C., Parada, C., this issue. Running the gauntlet: connectivity between natal and nursery areas for Pacific ocean perch (*Sebastes alutus*) in the Gulf of Alaska, as inferred from a biophysical individual-based model. Deep Sea Res. II.

Weingartner, T.J., Danielson, S.L., Royer, T.C., 2005. Freshwater variability and predictability in the Alaska Coastal Current. Deep Sea Res. II 52, 169-191. https://doi.org/10.1016/j.dsr2.2004.09.030.

Werner F.E., Quinlan, J.A., Lough, R.G., Lynch, D.R., 2001. Spatially-explicit individual based modeling of marine populations: a review of the advances in the 1990s. Sarsia 86, 411-421.

Yang, M-S. 1993. Food habits of the commercially important groundfishes in the GOA in 1990. U.S. Dep. Commer., NOAA Tech. Memo. NMFS-AFSC-22 150 p.

TABLES

Table 1a. Parameter values used in the arrowtooth flounder IBM (egg through small feeding preflexion larva stages).
Table 1b. Parameter values used in the arrowtooth flounder IBM (large feeding preflexion larva through benthic juvenile stages).
Table 2. Environmental indices considered as potential factors driving IBM-predicted successful settlement.
Table 3. Summary of the linear model analysis for the aggregate connectivity indices, as potentially related to the large scale (AO, PDO, and MEI) and ROMS-derived (CSF: cross-shelf flow) environmental indices. All models with 1 or 2 environmental indices as factors were examined; AICc was used to select the “best” model. Only models with adjusted $R^2 \geq 0.50$ are shown. ΔAICc is the change in AICc from the best 1-factor model to the best 2-factor model. The p-value, Pr(>F), for each model is an empirical family-wise p-value based on the simulating the model fitting process 10,000 times with normally-distributed random time series to obtain the cumulative distribution for the null model.

FIGURES

Fig. 1. Conceptual model for the arrowtooth flounder IBM. Life stages included in the IBM are: egg, small yolk sac larva, large yolk sac larva, small feeding (SFPr) pre-flexion larva, large feeding pre-flexion (LFPr) larva, postflexion larva, settlement-stage (settler) juvenile, and benthic juvenile. Larval drawing based on Matarese et al., 1989.

Fig. 2. a) Fits to temperature-dependent mean duration of arrowtooth flounder egg (sub-) stages, as characterized by Blood et al. (2007). b) Predicted development times, for different constant temperatures. Eggs hatch when the end of sub-stage 19 is reached.

Fig. 3. a): Mean abundance from Fisheries-Oceanography Coordinated Investigations (FOCI) ichthyoplankton tows that caught arrowtooth flounder eggs. b): Relative temporal pattern and weights for release of simulated eggs in the IBM.

Fig. 4. a) Time series from the 2015 GOA arrowtooth flounder stock assessment (Spies et al., 2015) for recruitment (lagged to spawning year; solid line) and spawning biomass (dotted line). b) Time series of R, ln(R) and ln(R/S), standardized as z-scores.

Fig. 5. Trajectories for successful (dark grey) and unsuccessful (light grey) individuals released in 2011 from spawning zones 2 (Sitka; upper row), 6 (Prince William Sound; center row), and 10 (Chirikof; bottom row). Left column: trajectories during the egg stage. Right column: trajectories during later stages.

Fig. 6. a) The fraction of individuals, by spawning area, successfully recruiting to nursery areas anywhere in the model domain. b) The average alongshore zone, by spawning area, to which successful individuals recruited (no individuals were successful from area 12).

Fig. 7. Median (lefthand plot) and root median square deviation (righthand plot) for the annual (1996-2011) connectivity matrices. Nursery zones are plotted from west to east (i.e., in descending order), except for Cook Inlet (alongshore zone 13).

Fig. 8. a) Principal component scores for each year associated with b) the first two EOFs of the connectivity matrices for 1996-2011. The two EOFs together explain 63% of the annual variance in connectivity.

Fig. 9. Time series for the fraction of individuals, by spawning area, successfully settling in nursery areas anywhere in the model domain (i.e., the $C_s(y)$). a) spawning zones 1-6; b) spawning zones 7-12. Note: y-axis scales are different.

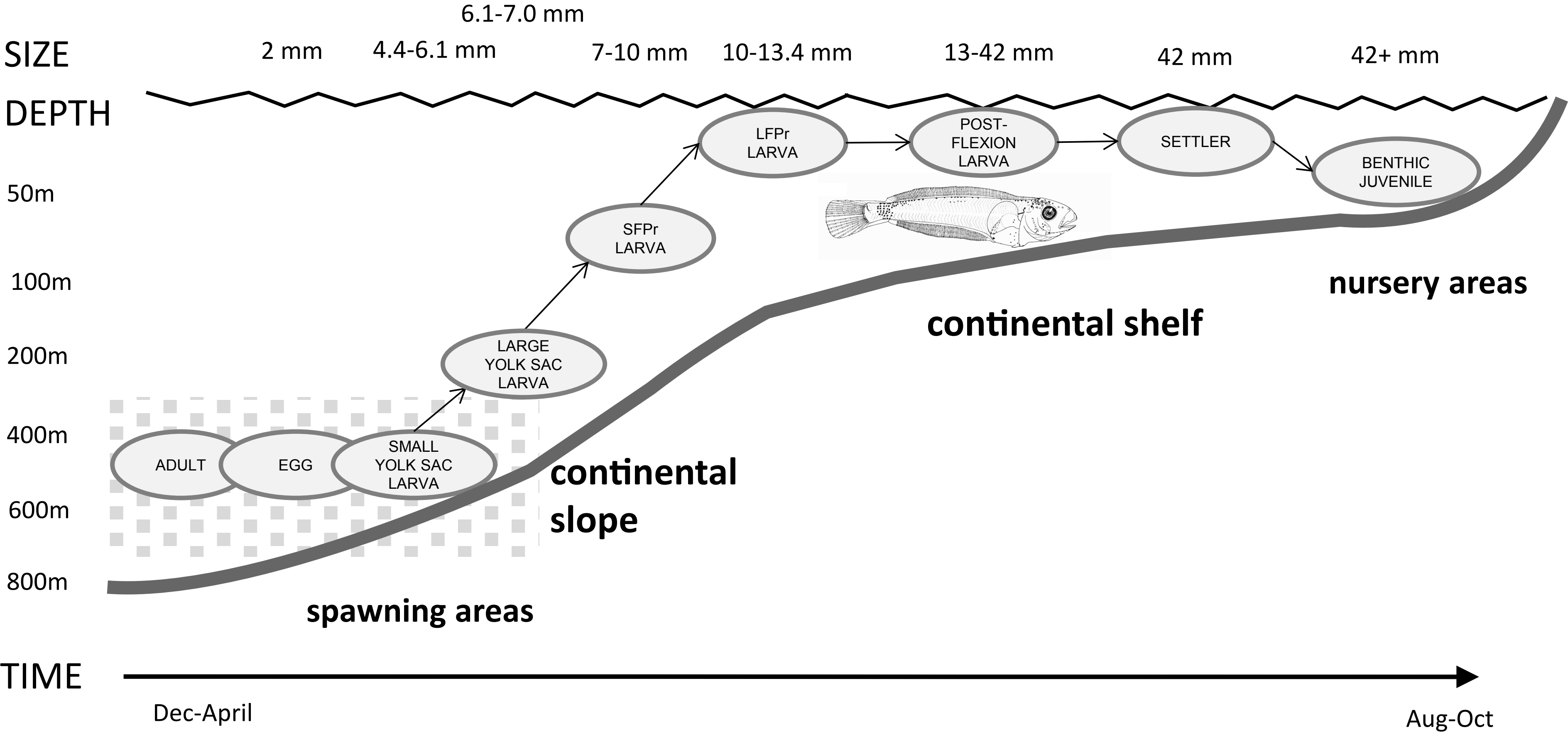
SIZE
2 mm
4.4-6.1 mm
6.1-7.0 mm
7-10 mm
10-13.4 mm
13-42 mm
42 mm
42+ mm
DEPTH
50m
100m
200m
400m
600m
800m
ADULT
EGG
SMALL YOLK SAC LARVA
LARGE YOLK SAC LARVA
SFPr LARVA
LFPr LARVA
POST-FLEXION LARVA
SETTLER
BENTHIC JUVENILE
continental slope
continental shelf
nursery areas
spawning areas
TIME
Dec-April
Aug-Oct

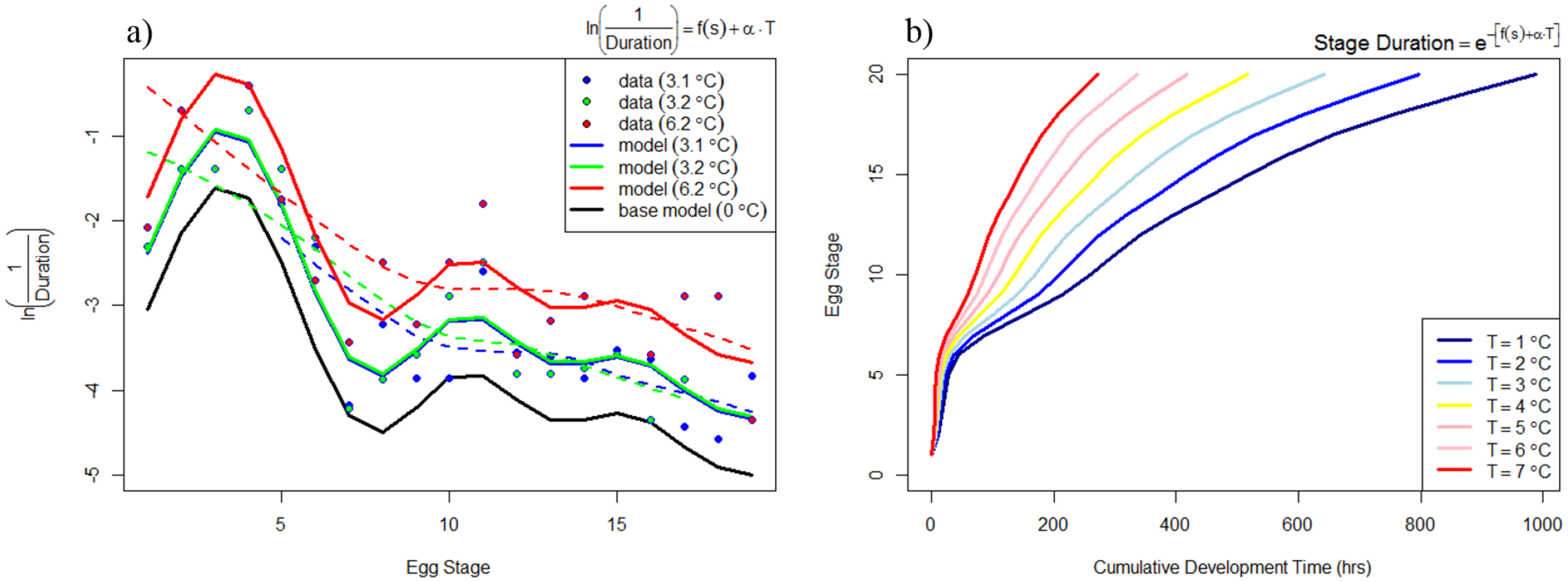
a)
$\ln\left(\frac{1}{\text{Duration}}\right) = f(s) + \alpha \cdot T$
data (3.1 °C)
data (3.2 °C)
data (6.2 °C)
model (3.1 °C)
model (3.2 °C)
model (6.2 °C)
base model (0 °C)
$\ln\left(\frac{1}{\text{Duration}}\right)$
Egg Stage
b)
Stage Duration $= e^{-[f(s)+\alpha \cdot T]}$
Egg Stage
Cumulative Development Time (hrs)
T = 1 °C
T = 2 °C
T = 3 °C
T = 4 °C
T = 5 °C
T = 6 °C
T = 7 °C

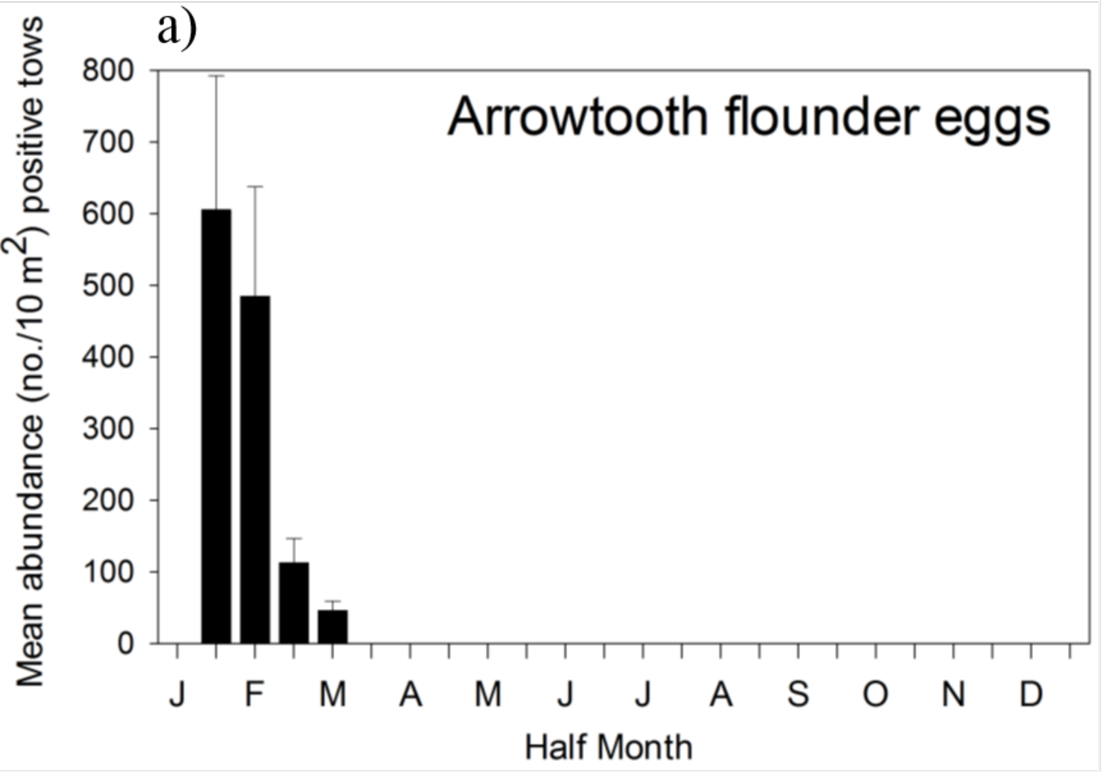
a)
Arrowtooth flounder eggs
Mean abundance (no./10 m2) positive tows
800
700
600
500
400
300
200
100
0
J F M A M J J A S O N D
Half Month

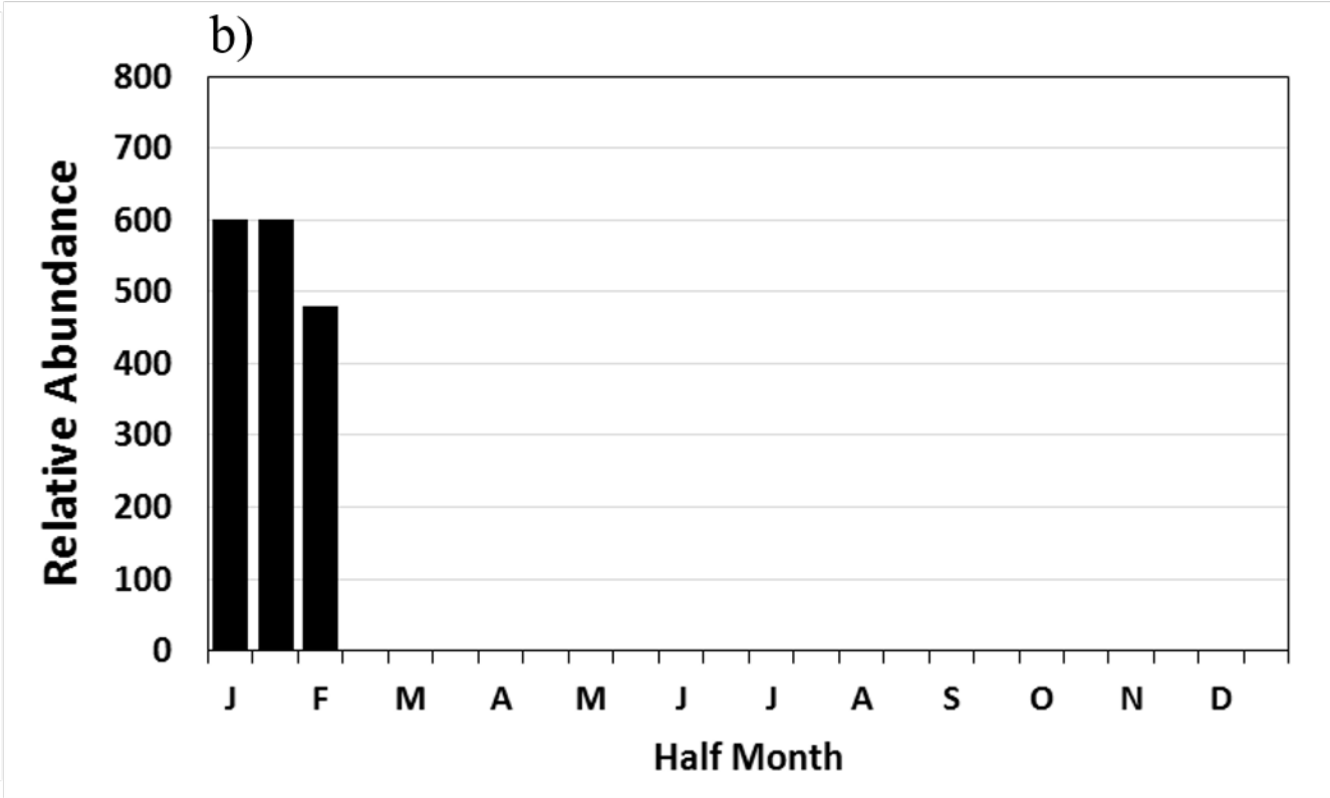
b)
Relative Abundance
800
700
600
500
400
300
200
100
0
J F M A M J J A S O N D
Half Month

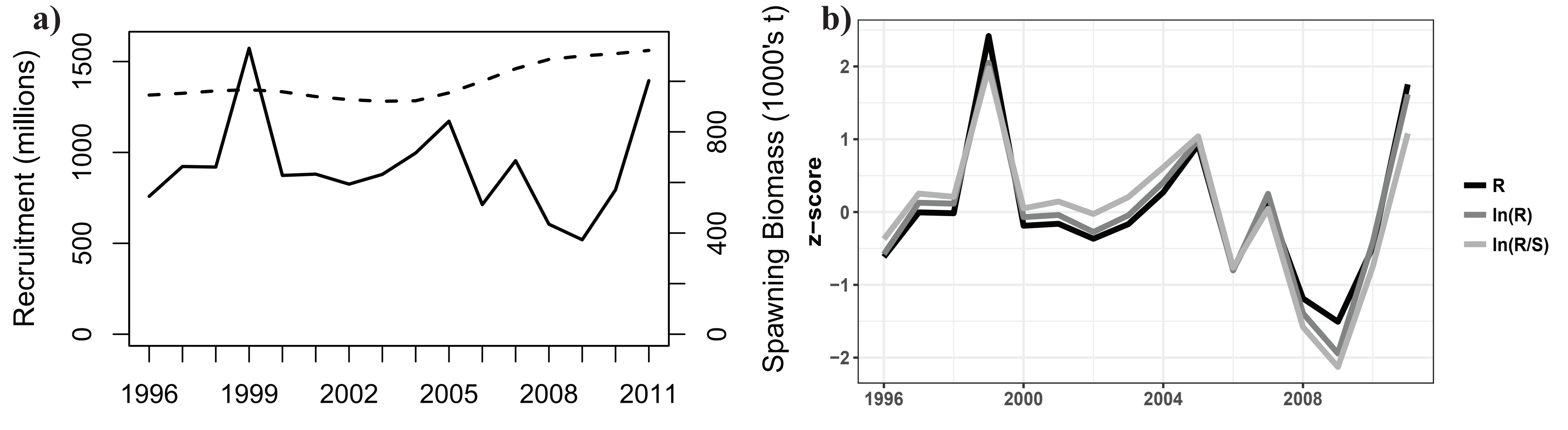

a)
Recruitment (millions)
Spawning Biomass (1000's t)
0
500
1000
1500
0
400
800
1996
1999
2002
2005
2008
2011
b)
z−score
2
1
0
−1
−2
1996
2000
2004
2008
R
ln(R)
ln(R/S)

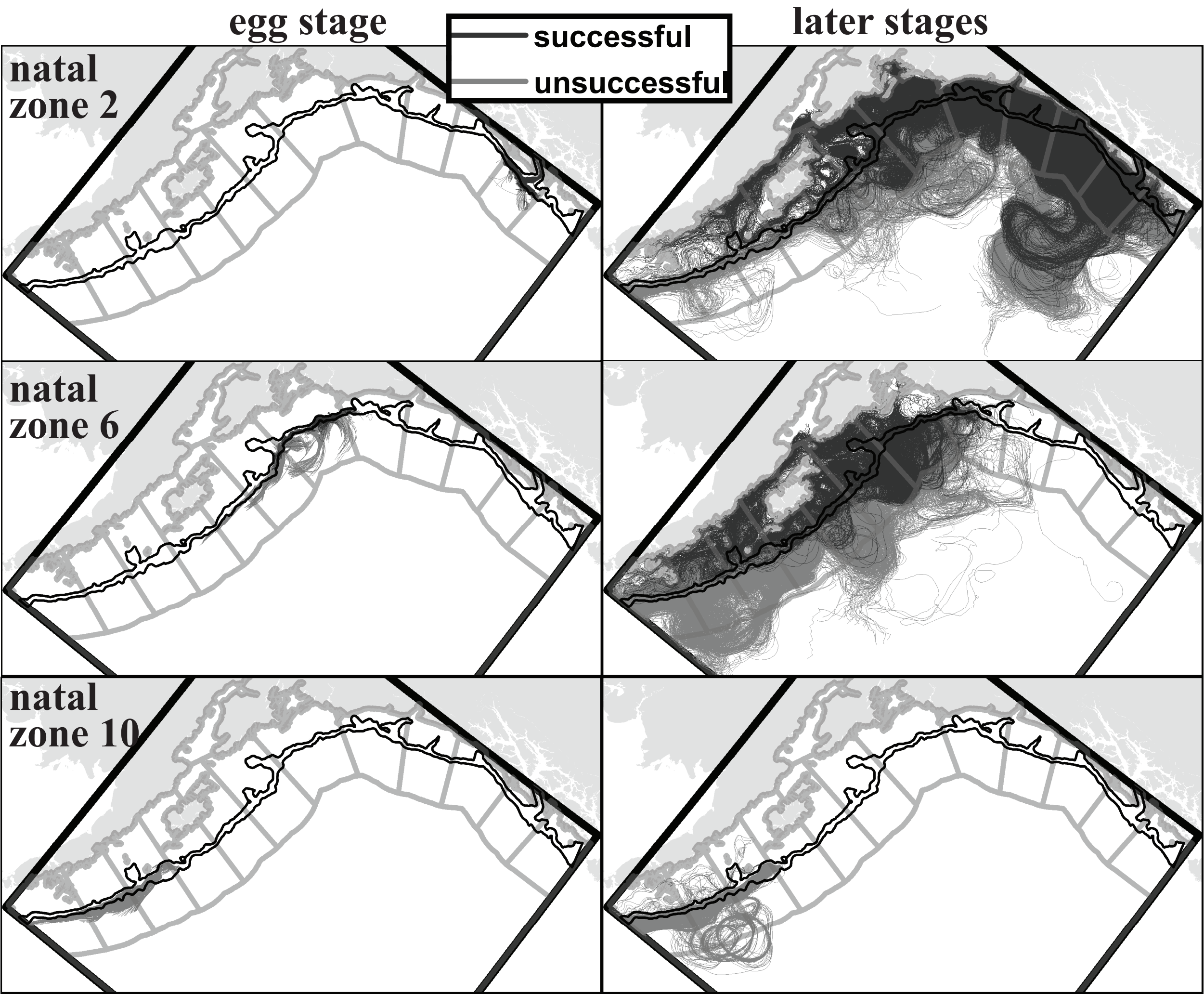
egg stage
later stages
successful
unsuccessful
natal zone 2
natal zone 6
natal zone 10

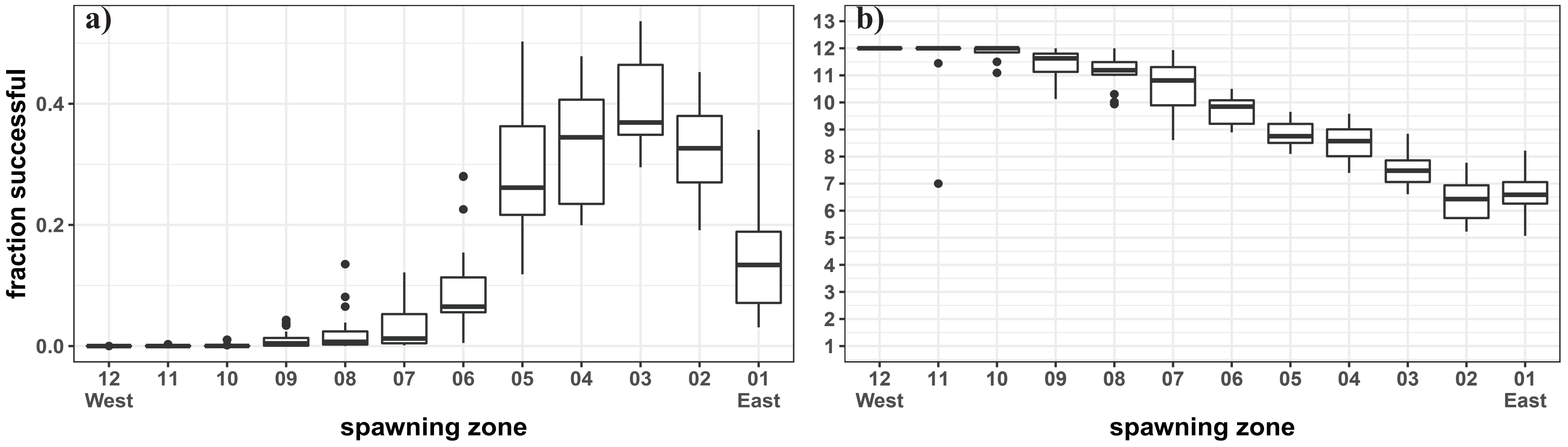
a)
fraction successful
0.0
0.2
0.4
12
West
11
10
09
08
07
06
05
04
03
02
01
East
spawning zone
b)
13
12
11
10
9
8
7
6
5
4
3
2
1
12
West
11
10
09
08
07
06
05
04
03
02
01
East
spawning zone

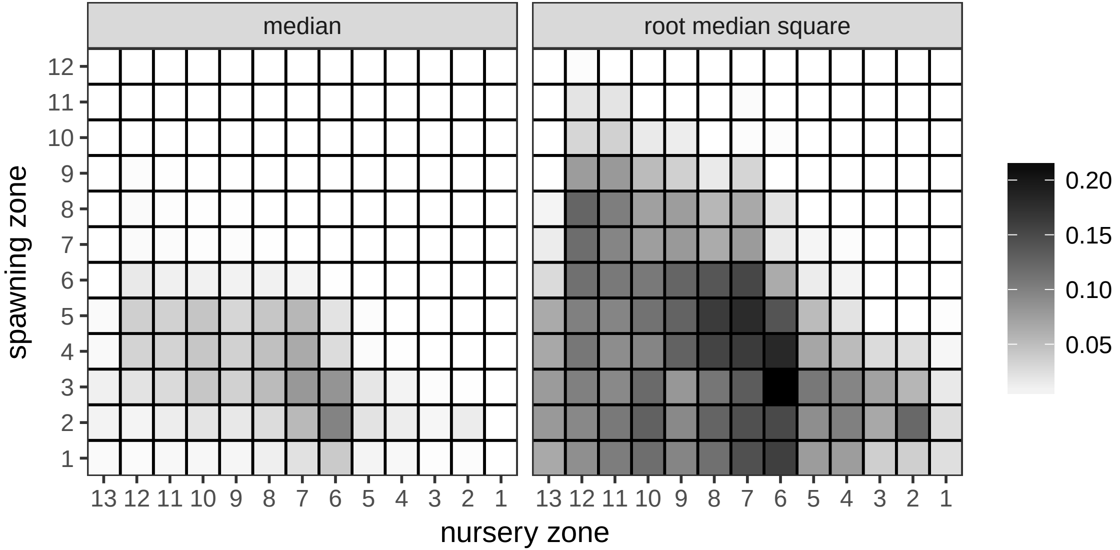

median
root median square
spawning zone
12
11
10
9
8
7
6
5
4
3
2
1
13 12 11 10 9 8 7 6 5 4 3 2 1
13 12 11 10 9 8 7 6 5 4 3 2 1
nursery zone
0.20
0.15
0.10
0.05

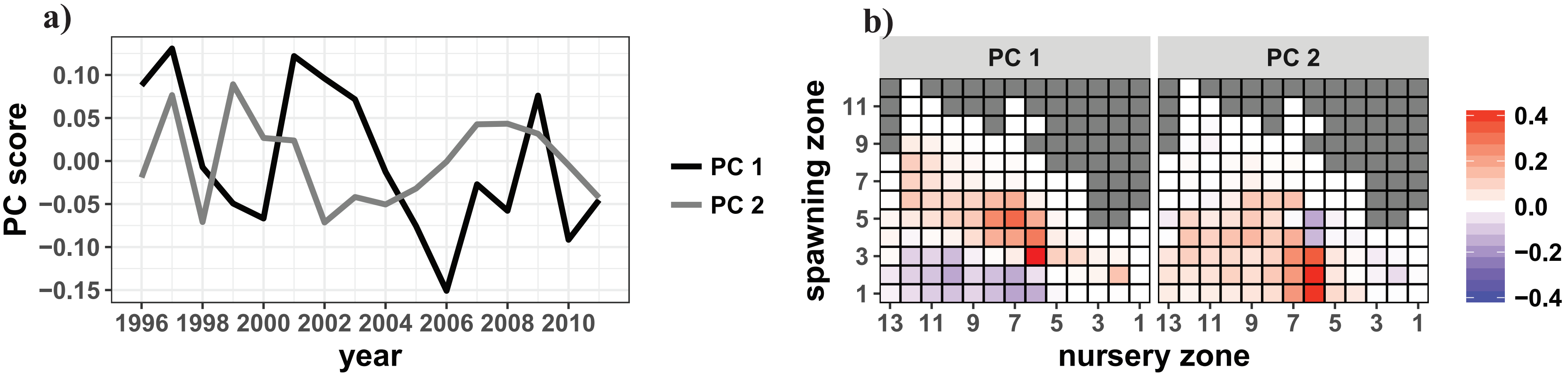
a)
PC score
0.10
0.05
0.00
−0.05
−0.10
−0.15
1996 1998 2000 2002 2004 2006 2008 2010
year
PC 1
PC 2
b)
PC 1
PC 2
spawning zone
11
9
7
5
3
1
13 11 9 7 5 3 1
nursery zone
0.4
0.2
0.0
−0.2
−0.4

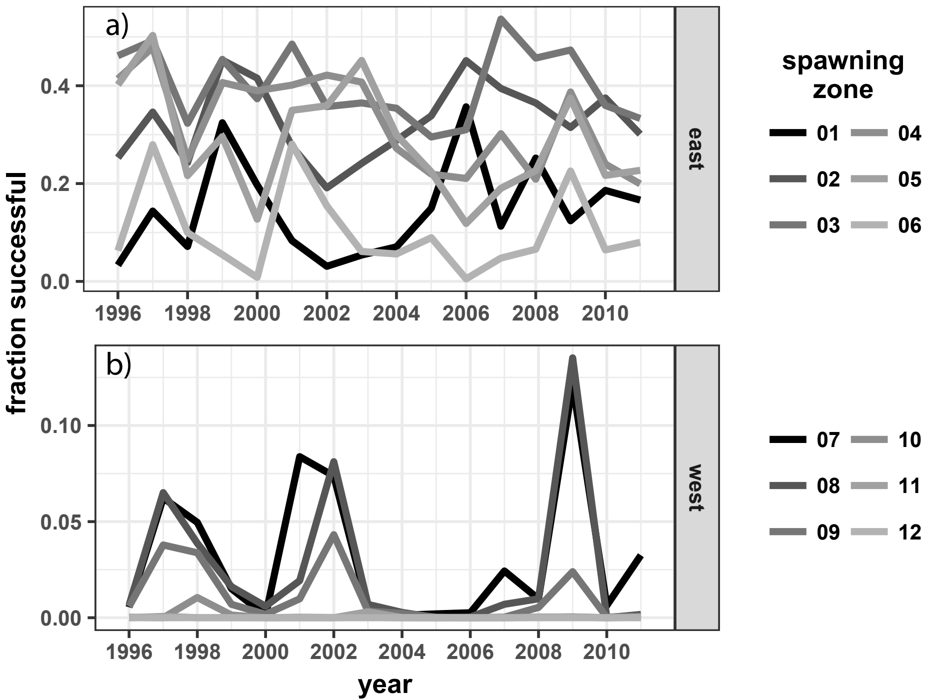
a)
b)
fraction successful
year
0.0
0.2
0.4
0.00
0.05
0.10
1996
1998
2000
2002
2004
2006
2008
2010
east
west
spawning zone
01
02
03
04
05
06
07
08
09
10
11
12

Table 1a. Parameter values used in the arrowtooth flounder IBM (egg through small feeding preflexion larva stages).

Life Stage	Parameter	Value	Units	Description	Based on
Egg Stage	d_{min}	300	m	min depth in water column	[1]
	d_{max}	600	m	max depth in water column	[1]
	b	1	mm/s	buoyancy rate	
	D_v	0.0001	m^2/s	vertical diffusivity	
	D_h	0.001	m^2/s	horizontal diffusivity	
Small Yolk Sac Larva	z_i	4.4	mm	initial size	[1]
	z_f	6.1	mm	final size	[1]
	g	0.008	day^{-1}	intrinsic growth rate	
	d_{min}	300	m	min depth in water column	[1]
	d_{max}	600	m	max depth in water column	[1]
	v_s	0.1	bl/s	vertical swimming speed	
	D_v	0.0001	m^2/s	vertical diffusivity	
	D_h	0.001	m^2/s	horizontal diffusivity	
Large Yolk Sac Larva	z_i	6.1	mm	initial size	[1]
	z_f	7	mm	final size	[1]
	g	0.008	day^{-1}	intrinsic growth rate	
	d_{min}	150	m	min depth in water column	
	d_{max}	300	m	max depth in water column	
	v_s	0.1	bl/s	vertical swimming speed	
	D_v	0.0001	m^2/s	vertical diffusivity	
	D_h	0.001	m^2/s	horizontal diffusivity	
Small Feeding Preflexion Larva	z_i	7	mm	initial size	[1], [2]
	z_f	10	mm	final size	[3]
	g	0.01	day^{-1}	intrinsic growth rate	[2]
	d_{min}	40	m	min depth in water column	[4]
	d_{max}	80	m	max depth in water column	[4]
	v_s	0.1	bl/s	vertical swimming speed	
	D_v	0.0001	m^2/s	vertical diffusivity	
	D_h	0.001	m^2/s	horizontal diffusivity	

[1]Blood et al., 2007; [2]Bouwens et al., 1989; [3]Matarese et al., 1989; [4]Doyle and Mier, submitted.

Table 1b. Parameter values used in the arrowtooth flounder IBM (large feeding preflexion larva through benthic juvenile stages).

Life Stage	Parameter	Value	Units	Description	Based on
Large Feeding Preflexion Larva	z_i	10	mm	initial size	[3]
	z_f	13.4	mm	final size	[1]
	g	0.01	day^{-1}	intrinsic growth rate	[2]
	d_{min}	10	m	min depth in water column	[4]
	d_{max}	30	m	max depth in water column	[4]
	v_s	0.1	bl/s	vertical swimming speed	
	D_v	0.0001	m^2/s	vertical diffusivity	
	D_h	0.001	m^2/s	horizontal diffusivity	
Postflexion Larva	z_i	13.4	mm	initial size	[1]
	z_f	42	mm	final size	[1], [2], [3]
	g	0.01	day^{-1}	intrinsic growth rate	[2]
	d_{min}	10	m	min depth in water column	[4]
	d_{max}	30	m	max depth in water column	[4]
	v_s	0.1	bl/s	vertical swimming speed	
	D_v	0.0001	m^2/s	vertical diffusivity	
	D_h	0.01	m^2/s	horizontal diffusivity	
Settlement-stage Juvenile	z_i	42	mm	initial size	[2]
	z_f	--	mm	final size	
	g	0.01	day^{-1}	intrinsic growth rate	[2]
	d_{min}	10	m	min depth in water column	[4]
	d_{max}	50	m	max depth in water column	[4]
	v_s	0.1	bl/s	vertical swimming speed	
	D_v	0.0001	m^2/s	vertical diffusivity	
	D_h	0.01	m^2/s	horizontal diffusivity	
	t_{max}	8	days	max. stage duration	
	d_{pna}	0-50	m	preferred nursery areas	[5]
	d_{ana}	50-150	m	alternative nursery areas	

[1]Blood et al., 2007; [2]Bouwens et al., 1989; [3]Matarese et al., 1989; [4]Doyle and Mier, submitted; [5]Abookire et al., 2001.

Table 2. Environmental indices considered as potential factors driving IBM-predicted successful settlement.

type	index	region	season	no. of indices
Large-scale indices	$\begin{Bmatrix} \text{AO} \\ \text{MEI} \\ \text{PDO} \end{Bmatrix}$	--	$\begin{Bmatrix} winter \\ spring \\ summer \\ fall \end{Bmatrix}$	12
ROMS-derived indices	cross-shelf flow (CSF)	$\begin{Bmatrix} \text{eastern GOA} \\ \text{central GOA} \\ \text{western GOA} \end{Bmatrix}$	$\begin{Bmatrix} winter \\ spring \\ summer \\ fall \end{Bmatrix}$	12

Table 3. Summary of the linear model analysis for the aggregate connectivity indices, as potentially related to the large scale (AO, PDO, and MEI) and ROMS-derived (CSF: cross-shelf flow) environmental indices. All models with 1 or 2 environmental indices as factors were examined; AICc was used to select the "best" model. Only models with adjusted $R^2 \geq 0.50$ are shown. $\Delta AICc$ is the change in AICc from the best 1-factor model to the best 2-factor model. The p-value, $\Pr(> F)$, for each model is an empirical family-wise p-value based on the simulating the model fitting process 10,000 times with normally-distributed random time series to obtain the cumulative distribution for the null model.

Connectivity Index Type	Zone/PC	Selected Covariate(s)	Coefficient	F value	$\Pr(> F)$	R^2	Adjusted R^2	AICc	$\Delta AICc$
$C_s\ (y)$	Zone 01	CSF eastern GOA-summer	0.747	9.99	0.30	0.61	0.55	35.8	-5.1
		CSF western GOA-winter	-0.577						
	Zone 06	CSF western GOA-spring	0.489	9.03	0.37	0.58	0.52	36.65	-3.6
		MEI-summer	0.556						
	Zone 07	MEI-spring	0.840	10.38	0.27	0.61	0.56	35.40	-4.6
		PDO-spring	-0.875						
	Zone 08	MEI-spring	0.938	16.29	0.07	0.71	0.67	30.90	-10.4
		PDO-spring	-0.912						
	Zone 09	MEI-spring	1.06	18.28	0.05	0.74	0.70	29.64	-6.7
		PDO-spring	-0.61						
	Zone 10	MEI-spring	0.98	16.78	0.06	0.72	0.68	30.58	-8.6
		PDO-fall	-0.68						